Transmissive Diffractive Optical Elements Based on Cholesteric Liquid Crystal

Taiki Yoda, Ayaka Higuchi**, Koichi Igeta**, Kasumi Hase**, Junji Kobashi**, Yasushi Tomioka**, Shinichiro Oka**, Hiroyuki Yoshida**

*School of Engineering, Kwansei Gakuin University, Hyogo, Japan

**Japan Display Inc., Chiba, Japan

Abstract

We propose a transmissive diffractive optical element based on cholesteric liquid crystals. The proposed device shows wavelength selective stemming from the Bragg reflection of cholesteric liquid crystals and is in sharp contrast to conventional liquid crystal diffractive optical elements based on the Pancharatnam-Berry phase. Since the Bragg diffraction is wavelength selective, the device is potentially attractive for the dispersion control of transmissive diffractive optical elements.

Author Keywords

Liquid crystal; Polarization volume hologram; VR/AR

1. Objective and background

Holographic optical elements (HOEs) made of liquid crystals (LCs) are promising for realizing thin and light-weight diffractive optical elements (DOEs). Recent works related to LC-based transmissive DOEs have mainly focused on optical elements based on the Pancharatnam-Berry (PB) phase. Compared to other DOEs, LC-based PB optical elements offer several advantages such as high diffraction efficiency and easy fabrication. However, the PB-based optical element has some drawbacks for practical applications. First, the PB-based DOE is essentially chromatic because the diffraction angle depends on the incident wavelength. For future applications, the correction of chromatic aberration is critical because chromatic aberration reduces the quality of a lens. One way to reduce the chromatic aberration is to adjust the diffraction angle for each wavelength. However, it is difficult to adjust the diffraction angle for each wavelength by using conventional PB-based DOEs. Next, the diffraction efficiency of PB-based DOEs decreases as the period becomes shorter [1] because the theoretical analysis of PB-based diffraction relies on the paraxial approximation [2,3]. Because a short period is generally required to obtain a large diffraction angle, PB-based DOEs work efficiently only for small diffraction angles.

In this presentation, we propose a transmissive DOE with diffraction property different from the PB-based DOE. The proposed device consists of a stack of two HOEs based on cholesteric liquid crystals (CLCs). CLC-based HOEs diffract incident light only when its wavelength is within the photonic band gap. This wavelength selectivity stems from Bragg diffraction. While CLC-based HOEs are commonly used in reflective grating and lens [4], we find that the multilayer of two HOEs works as transmissive DOEs with characteristic wavelength selectivity. Because our device relies on Bragg diffraction, the diffraction property is largely different from the PB-based DOEs. The light incident on the multilayer undergoes the Bragg diffraction twice, which achieves transmissive diffraction with wavelength selectivity. The operation wavelength and the diffraction angle of our device are tuned by the pitch and the period of a HOE. For example, we can design three DOEs which diffract only blue, green, and red light. Moreover, their diffraction angles can be designed to be the same. Cascading these DOEs potentially leads to achromatic DOEs. Improving chromatic aberration will benefit many applications such as AR/VR displays.

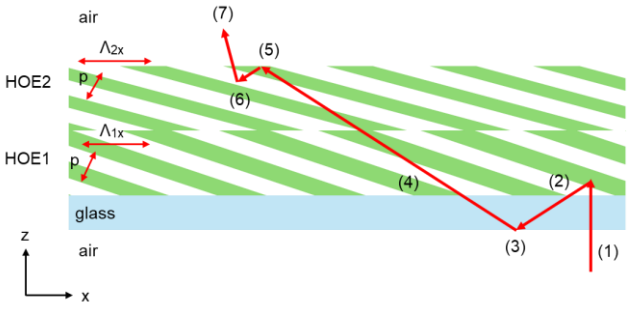

Figure 1. Schematic illustration of multilayer and its operation principle.

2. Theoretical analysis

We consider a stack of two HOEs consisting of patterned cholesteric liquid crystals. The multilayer is on a glass substrate. The schematic illustration is shown in Fig. 1. The green and white lines in the HOEs schematically represents the isophase surface of the director of liquid crystals. The two HOEs are characterized by structural parameters, namely the pitch p and grating period Λ_x. We analyze the diffraction property of the multilayer by using the geometrical optics analysis. Here we assume that the structure is invariant in the y direction. The operation mechanism of the multilayer is summarized as follows. (1) The circularly polarized light is incident from the lower air region, and (2) the incident light is diffracted by HOE1. If Λ_{1x} is short so that the diffraction angle is greater than the critical angle of the interface between the substrate and lower side, (3) the diffracted light is reflected by the total internal reflection. (4) The reflected light re-enters HOE1 with an oblique angle, and the entered light passes through HOE1 and HOE2. (5) The light is reflected by total internal reflection at the interface between HOE2 and the upper air cladding. (6) The reflected light is diffracted by HOE2, and then (7) the diffracted light exits from HOE2 into the upper side. The transmitted angle θ_t is calculated from the geometrical optics analysis, and it is expressed as

$$\sin\theta_t - \sin\theta_i = \frac{\lambda}{\Lambda_{2x}} - \frac{\lambda}{\Lambda_{1x}}, \tag{1}$$

where θ_i is the incident angle, λ is the incident wavelength, Λ_{1x} (Λ_{2x}) is the period of HOE1 (HOE2), and α_1 is the slanted angle of the isophase surface of HOE 1. Equation (1) holds only when the incident light is diffracted by both HOEs. Therefore, the bandwidth of two HOEs must overlap.

The multilayer works as a transmissive grating when Λ_{1x} and Λ_{2x} are constants which is independent of position x. We can also

ISSN 0097-996X/25/5602-1286-$1.00 © 2025

achieve a transmissive lens by choosing Λ_{2x} as

$$\frac{1}{\Lambda_{2x}} = \frac{1}{\Lambda_{1x}} - \frac{1}{\lambda_t}\frac{x - x_0}{\sqrt{(x - x_0)^2 + f^2}}. \quad (2)$$

Where λ_t is the target wavelength, and f is the focal length, and x_0 is the shift of the director in the x direction. When Λ_{2x} satisfies Eq. (2), the transmitted angle under normal incidence is given by

$$\sin\theta_t = -\frac{\lambda}{\lambda_t}\frac{x - x_0}{\sqrt{(x - x_0)^2 + f^2}}. \quad (3)$$

Equation (3) is consistent with the lens formula except for the shift x_0 in the x direction, which means that the normal incident light with $\lambda = \lambda_t$ is focused at $z = f$. The focal spot shifts in the x direction by x_0 [5].

3. Numerical calculation

To verify the operation of proposed multilayer structure, we numerically evaluate the diffraction property of the multilayer by using finite-difference time-domain (FDTD) method. In this presentation, we demonstrate diffractive optical elements which diffract light with wavelengths around 550 nm. In numerical calculation, the ordinary refractive index n_{io} and extraordinary one n_{ie} are set to $n_{1o} = n_{2o} = 1.58$ and $n_{1e} = n_{2e} = 1.73$. We assume that the directors of two HOEs have slanted structure which is expressed by

$$n_i = (\cos\varphi_i \cos\alpha_i, \sin\varphi_i, -\cos\varphi_i \sin\alpha_i)$$

where φ_i is the phase of the director, and $\alpha_i = \sin^{-1}(p_i/2\Lambda_{ix})$ is the slanted angle of the director. The pitch and thicknesses of the HOEs are fixed at 362 nm and 3 μm, respectively. The refractive index and thickness of a glass substrate is 1.52 and 1 μm, respectively. In all numerical calculations, the incident polarization is right circularly polarized (RCP).

3.1. Grating

We first demonstrate a wavelength-selective transmissive grating with $\Lambda_{1x} = 460$ nm and $\Lambda_{2x} = 420$ nm. In this case, the diffraction angle of the m-th order diffraction is given by $\theta_{t,m} = \sin^{-1}(m\lambda/\Lambda)$ with $\Lambda = 9660$ nm, and the diffraction order m ranges from -27 to 27. The transmissive diffraction efficiency for each diffraction order under normal incidence is shown in Fig. 2(a). The transmission power is mostly concentrated in the zeroth and second order diffraction. The second order diffraction occurs at wavelengths around 550 nm while no diffraction occurs at other wavelengths. This result clearly demonstrates that the multilayer structure diffracts only light at specific wavelengths. The wavelength range of the second order diffraction corresponds to the diffraction bandwidth of HOE1. We also decompose the diffraction efficiency into right-circular and left-circular components (Fig. 2(b)). The polarization of the diffracted light is mostly RCP, which means that the incident polarization is preserved when the incident light is diffracted. This is a contrast to the case of a PB grating because a PB grating flips the handedness of incident circular polarization.

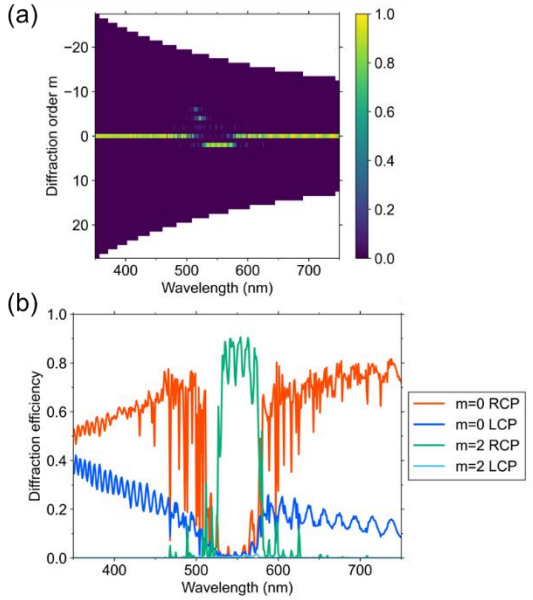

Figure 2. (a) Transmissive diffraction efficiency for all diffraction orders. (b) RCP and LCP components of diffraction m=0 and m=2.

3.2. Lens

Next, we numerically demonstrate a wavelength-selective transmissive lens. From Eqs. (2) and (3), the director of HOE2 should be chosen as

$$\varphi_2 = \frac{\pi}{\Lambda_{1x}}(x - x_0) - \frac{\pi}{\lambda_t}\left[\sqrt{(x - x_0)^2 + f^2} - f\right] + \frac{\pi}{\Lambda_{2z}}z. \quad (4)$$

In the numerical calculation, we use the following parameters: $\Lambda_{1x} = 460$ nm, $f = 100$ μm, $\lambda_t = 550$ nm, and $x_0 = -24$ μm. The width of the multilayer is 150 μm, and the radium of an incident Gaussian beam is 30 μm. Figure 3(a) shows the angle dependence of the far field intensity at $\lambda = 450$ nm, 550 nm, and 650 nm. At λ =550 nm, the diffraction angle ranges from $-30°$ to $30°$ in the lens plane. On the other hand, the incident light is not diffracted at other wavelengths. The intensity distribution of the far field in the xz plane is shown in Fig. 3(b). We can confirm that the incident light with $\lambda = 550$ nm is focused around $z = 100$ μm

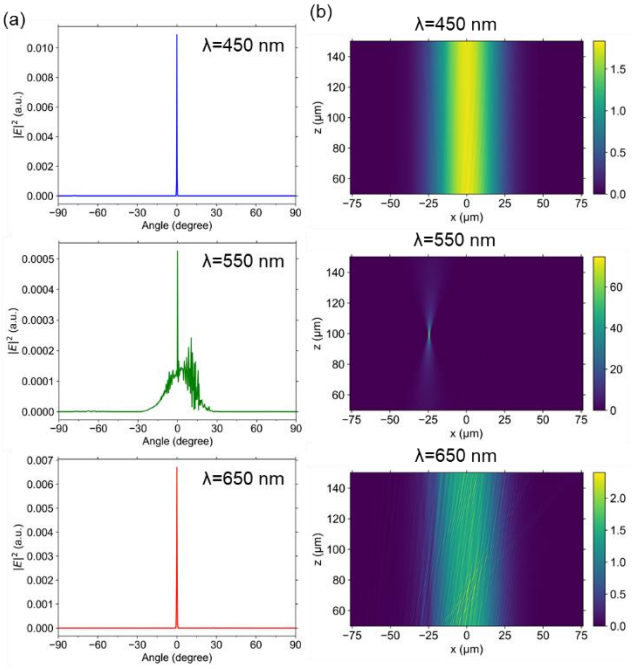

Figure 3. Diffraction property of wavelength-selective lens. (a) Angle dependence of far field intensity at $\boldsymbol{\lambda = 450}$ nm, $\boldsymbol{\lambda = 550}$ nm, and $\boldsymbol{\lambda = 650}$ nm. (b) Focusing property of multilayer in the xz plane.

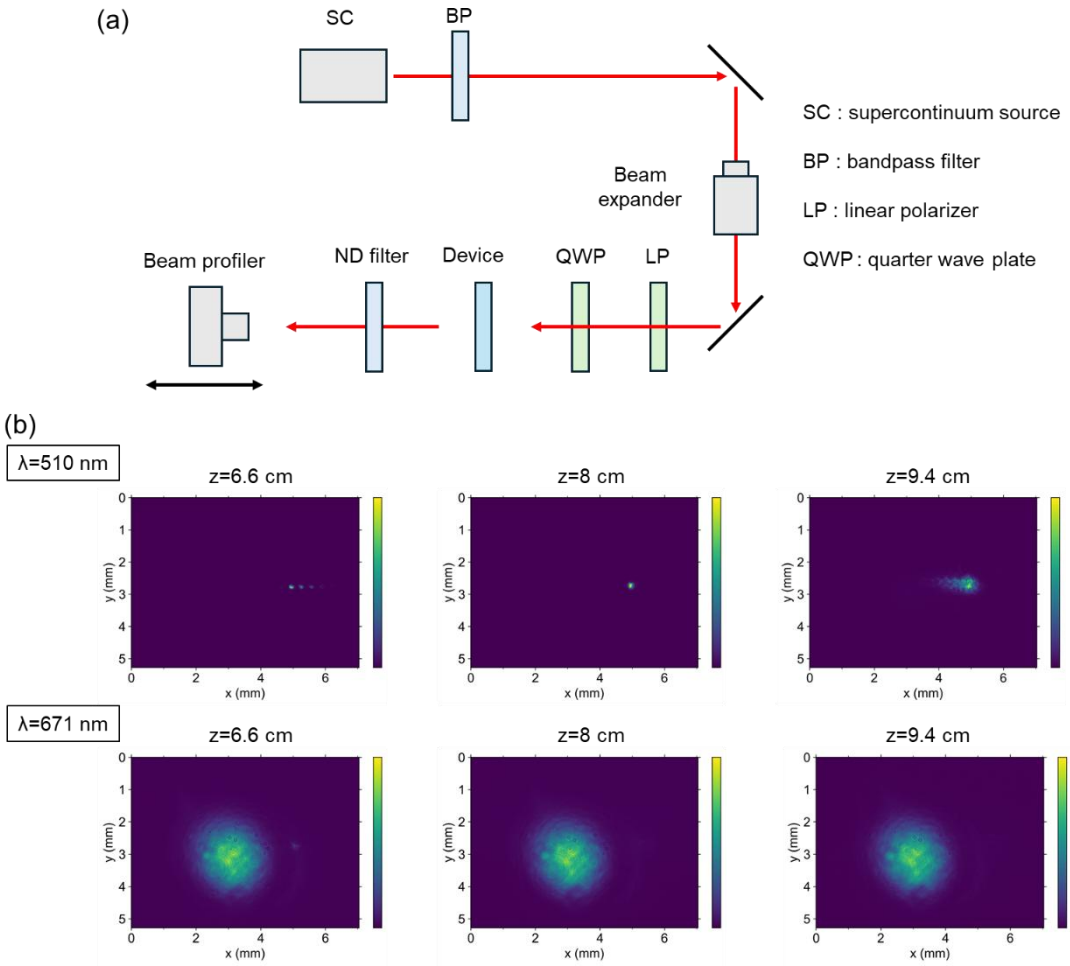

Figure 4. (a) Experimental setup for characterization of lens. (b) Focal spot intensity profiles at wavelengths of 510 nm and 671 nm.

from the surface of the multilayer. In contrast, the incident light with $\lambda = 450$ nm and 650 nm are not focused and propagates straight after the transmission.

4. Experimental result

We fabricated a multilayer structure of two HOEs to experimentally demonstrate the focusing property of proposed structure. The fabrication process of bottom (HOE1) and top (HOE2) layers is as follows. To fabricate a multilayer, we first fabricated each layer separately. We spin-coated a photoalignment layer on grass substrates with 0.7 mm thickness. Then, the photoalignment layer was exposed by two circularly polarized beams with opposite handedness to create a periodic modulation of the orientation direction of molecules. HOE1 was exposed by using two collimated beams. HOE2 was exposed by using a collimated beams and a beam passing through a convex lens, which acts as a template to impart a paraboloidal diffraction profile. The focal length of the template lens is 15 cm, and the lens is placed 27 cm away from the sample. Next, CLC layers were spin-coated and polymerized to obtain a solid film. After polymerization, we separated HOE2 from the substrate and finally HOE2 was attached onto HOE1.

The experimental setup for device characterization is shown in Fig. 4(a). The fabricated sample is illuminated by an RCP beam and the transmitted light is captured by a beam profiler on a translation stage. The diameter of the incident beam in the x direction is approximately 1.6 mm, and the incident beam incident at the center of the sample. Figure 4(b) shows several images at several distances from the sample. For $\lambda = 510$ nm, several ghost images occur at $z = 6.6$ cm and $z = 9.4$ cm. The incident beam is focused around $z = 8$ cm, and the ghost images merges at $z = 8$ cm. The diameter of the focal spot in the x direction is approximately 0.19 mm. We note that the focused beam shifts 1.9 mm in the x direction compared to the beam without the sample. The walk-off of the incident beam can also be observed in the numerical calculation (Fig. 3). In contrast, the incident beam is not focused at $\lambda = 671$ nm. This experimental result demonstrates that the proposed multilayer structure works as a wavelength selective diffractive lens.

5. Discussion and Conclusion

Recently, an achromatic LC-based DOE with cascaded three layers lens has been proposed [6,7], while our proposal is based on different mechanism. Because our structure utilizes the Bragg diffraction, there may be some advantages such as wavelength selectivity, diffraction efficiency, and large diffraction angle.

In conclusion, we propose a transmissive DOEs consisting of a multilayer of patterned CLC. The proposed multilayer structure shows wavelength selective transmissive diffraction based on the Bragg diffraction of CLCs. It is difficult to achieve such

wavelength selectivity by using conventional LC-based DOEs. The operation wavelength, operation bandwidth and diffraction angle can be tuned by the refractive index, pitch, and in-plane periodicity. Our proposed device has the potential to improve chromatic aberration by stacking multilayers with different operation wavelength but same diffraction angle.

6. Acknowledgement

This work was supported by JST A-STEP Grant Number JPMJTR222E and JSPS KAKENHI Grant Number JP23K26573. The authors thank JNC Corporation for providing the materials.

7. References

1. Oh C, Escuti MJ. Numerical analysis of polarization gratings using the finite-difference time-domain method. Phys. Rev. A 2007; 76: 043815.
2. Nikolova N, Todorov T. Diffraction Efficiency and Selectivity of Polarization Holographic Recording. Opt. Acta 1984; 31: 579.
3. Gori F. Measuring Stokes parameters by means of a polarization grating. Opt. Lett. 1999; 24: 584.
4. Kobashi J, Yoshida H, Ozaki M. Planar optics with patterned chiral liquid crystals 2016; 10: 389.
5. Yin K, He Z, Wu S-T. Reflective Polarization Volume Lens with Small f-Number and Large Diffraction Angle. Adv. Opt. Mater. 2020, 8, 2000170.
6. Luo Z, Li Y, Semmen J, Rao Yi, Wu S-T. Achromatic diffractive liquid-crystal optics for virtual reality displays. Light: Science & Applications 2023; 12: 230.
7. Ding Y, Huang X, Ma Y, Li Y, Wu S-T. High-efficiency RGB achromatic liquid crystal diffractive optical elements. Opto-Electronic Advances 2025; 8, 240181.